Marangoni-driven convection around exothermic autocatalytic chemical fronts in free-surface solution layers

L. Rongy, P. Assemat, and A. De Wit

Citation: Chaos **22**, 037106 (2012); doi: 10.1063/1.4747711
View online: http://dx.doi.org/10.1063/1.4747711
View Table of Contents: http://chaos.aip.org/resource/1/CHAOEH/v22/i3
Published by the American Institute of Physics.

Marangoni-driven convection around exothermic autocatalytic chemical fronts in free-surface solution layers

L. Rongy, P. Assemat, and A. De Wit
Nonlinear Physical Chemistry Unit, Service de Chimie Physique et Biologie Théorique, Faculté des Sciences, Université Libre de Bruxelles (ULB), CP 231, 1050 Brussels, Belgium

(Received 2 May 2012; accepted 9 August 2012; published online 28 September 2012)

Gradients of concentration and temperature across exothermic chemical fronts propagating in free-surface solution layers can initiate Marangoni-driven convection. We investigate here the dynamics arising from such a coupling between exothermic autocatalytic reactions, diffusion, and Marangoni-driven flows. To this end, we numerically integrate the incompressible Navier-Stokes equations coupled through the tangential stress balance to evolution equations for the concentration of the autocatalytic product and for the temperature. A solutal and a thermal Marangoni numbers measure the coupling between reaction-diffusion processes and surface-driven convection. In the case of an isothermal system, the asymptotic dynamics is characterized by a steady fluid vortex traveling at a constant speed with the front, deforming and accelerating it [L. Rongy and A. De Wit, J. Chem. Phys. **124**, 164705 (2006)]. We analyze here the influence of the reaction exothermicity on the dynamics of the system in both cases of cooperative and competitive solutal and thermal effects. We show that exothermic fronts can exhibit new unsteady spatio-temporal dynamics when the solutal and thermal effects are antagonistic. The influence of the solutal and thermal Marangoni numbers, of the Lewis number (ratio of thermal diffusivity over molecular diffusivity), and of the height of the liquid layer on the spatio-temporal front evolution are investigated. © *2012 American Institute of Physics*. [http://dx.doi.org/10.1063/1.4747711]

As a chemical reaction induces changes in the temperature and in the composition of the reactive medium, it can modify the properties of the solution (density, viscosity, surface tension) and thereby trigger convective motions, which in turn affect the reaction. Such a coupling can typically be observed around reactive interfaces in liquid solutions. Two classes of convective flows are then commonly developing in solutions open to air, namely Marangoni flows arising from surface tension gradients and buoyancy flows driven by density gradients. As both flows can be induced by compositional changes as well as thermal changes and in turn modify them, the resulting experimental dynamics are often complex. The purpose of our study is to gain insight into these intricate dynamics thanks to the theoretical analysis of model systems where only one type of convective flow is present. We address here the dynamics of an exothermic autocatalytic front propagating in the presence of Marangoni flows, when the density remains uniform. The surface tension gradient across the front has both a thermal component linked to the exothermicity of the reaction and a solutal component arising from the change in the chemical composition during the reaction. We show that the thermal effects modify the properties of the isothermal system and that new dynamics such as oscillations of the concentration field can be observed when the solutal and thermal effects act antagonistically on the surface tension, provided that they act on different length scales.

I. INTRODUCTION

Autocatalytic chemical reactions maintained far from thermodynamic equilibrium are the source of a wide variety of complex dynamic behaviors. Amongst the various observed phenomena (multistability, oscillations, spatio-temporal chaos, etc.), the generation of dissipative structures in spatially extended open systems has drawn much interest.[2] Propagating chemical fronts converting a reaction mixture from one state to another state are well-known examples of self-organized structures resulting from the interplay between autocatalytic chemical reactions and diffusion. Their properties have extensively been analyzed theoretically and related experiments have been carried out typically in gels, inert with respect to the reactants, to avoid any convection.[3–5] Although chemical fronts usually propagate at a constant speed, fronts of known autocatalytic reactions such as the iodate-arsenous acid (IAA) reaction or traveling waves have, however, been noted to propagate with larger velocities and be deformed in liquid solutions.[4,6–18] This is now understood to be due to natural convection initiated by the spatio-temporal distribution of heat and mass across the front through a change in the physical properties of the solution (density, viscosity, or surface tension). The evolution of the system is then determined by an intricate interplay between chemical and transport processes, namely, diffusion and convective motions of the fluid.

In vertical systems filled with the reactive solution, density differences can trigger buoyancy convection leading for instance to fingering of the interface between the reactants and the products if the denser solution lies on top of the less dense one in the gravity field.[19–24] Various scenarios of buoyancy-driven instabilities have been shown to arise from the combination of solutal and thermal contributions to the density difference across the front.[9,25–29] In horizontal geometries, the situation can become even more complicated if

the solution is open to air. Indeed, besides possible density gradients, there is an additional source of fluid motions, the Marangoni effects triggered by surface tension gradients at the air-liquid interface. Both sources of convection can therefore compete in such systems. Because of the usually large number of effects involved (nonlinear reaction kinetics, variations of density, or surface tension generated by both compositional and heat effects), model systems where only one type of convective flow is interacting with the reactive and diffusive processes are needed to gain insight into the mechanisms at the source of the system dynamics in horizontal aqueous layers.

In closed horizontal solution layers (no surface open to air), convection triggered by the density jump across a propagating front has been shown both experimentally[30–34] and numerically[35–41] to deform and to speed up this front in isothermal conditions. When the reaction is exothermic, the combination of solutal and thermal density changes comes into play and has been noted to affect for instance the propagation of polymerization fronts in horizontal layers[42,43] and to result in new dynamical behaviors for the case of chemical fronts of the chlorite-tetrathionate (CT) reaction[44–46] and of the IAA reaction.[47]

On the other hand, the opposite limit case of pure Marangoni flows affecting the propagation of chemical fronts in the absence of density changes has been relatively less investigated except for the case of surface reactions.[48,49] In the particular case of the Belousov-Zhabotinskii (BZ) reaction, numerical integrations of the Oregonator model equations coupled to the Navier-Stokes equations have allowed the comparison between Marangoni and buoyancy-driven effects on the dynamics of pulse waves.[50] In particular, using a similar model has allowed to relate the presence of oscillating flows observed during the propagation of BZ spiral waves[14] to Marangoni effects induced by the surface activity of bromomalonic acid.[51]

Similarly to the BZ reaction which is a canonical model for the study of pulse and spiral waves, the IAA reaction possesses rich dynamic behaviors. In a batch reactor, this reaction exhibits the so-called "clock dynamics," i.e., the reaction undergoes a sudden single switch from the reactants towards the products after an induction period depending on the initial concentrations. This reflects the slow growth of the autocatalytic species concentration up to a certain value and then its rapid production until the limiting reactant is completely consumed. The conversion fronts of the IAA reaction in spatially extended systems can be described in some concentration ranges of the reactants by a one-variable reaction-diffusion equation possessing an analytical solution,[3,52,53] which makes the IAA reaction a suitable model for the study of conversion fronts. This analytical solution is in good agreement with experimental studies carried out in gels (e.g., Ref. 54) but, as mentioned earlier, convection can affect the dynamics and propagation speeds of these fronts in aqueous solutions.[9,19,20,27,33,41,47,52] As discussed above, the complexity of such experimental systems arises from the fact that it is not always trivial to discriminate between surface tension-driven and buoyancy-driven convection.

In this general context, we have analyzed model systems where only one type of convective flow is interacting with the reactive and diffusive processes in horizontal geometries. We have first considered the propagation of an autocatalytic conversion front in the presence of pure solutal Marangoni convection[1,55] and pure solutal buoyancy convection,[39] showing that the system attains an asymptotic dynamics characterized by a steady fluid vortex traveling at a constant speed with the front. In both cases, the front is deformed across the layer and propagates faster than in the absence of natural convection. The propagation speed, the front deformation, and the intensity of the fluid flow increase, in both cases, with the layer thickness and with the strength of the coupling between reaction-diffusion (RD) processes and convection, measured by a Marangoni and a Rayleigh number, M and Ra, respectively. However, the two systems present important differences too, which could help differentiate experimentally between Marangoni and buoyancy convection in solution layers with an open surface.[39]

We have next considered the dynamics of an exothermic front propagating in covered layers in the presence of pure buoyancy convection alone showing important modifications in the system with regard to the isothermal dynamics.[44,56] We have investigated two different situations: the first one where the solutal and thermal effects act cooperatively to decrease the density of the solution during the reaction, and the second one where they act antagonistically. In the latter case, temporal oscillations of the concentration, temperature, and velocity fields can occur in a frame of reference moving at a constant speed with the front.

It is the objective of this paper to complement those previous studies by considering heat effects on the propagation of a chemical front in the presence of pure Marangoni convection. Our goal is on one hand to analyze to what extent thermal effects modify the dynamic properties of the pure solutal Marangoni effects.[1,55] On the other hand, we plan to see whether the combination of solutal and thermal effects can provide more complex Marangoni dynamics as it has been shown to do in the buoyancy case[44,56] and eventually to compare Marangoni and buoyancy-driven flows around exothermic fronts.

The article is therefore organized as follows. In Sec. II, we introduce the governing equations of the study and briefly review the numerical technique used to compute the solutions. Our results are presented and discussed in Sec. III and we conclude our work in Sec. IV.

II. MODEL

A. Governing equations and dimensionless parameters

We study the propagation of an autocatalytic front in a horizontal, two-dimensional solution layer of length L_x and height L_z (see Figure 1). An exothermic autocatalytic reaction takes place in the solution according to the global irreversible kinetics A+ 2C → 3C. When coupled to diffusion, this kinetics can give rise to the propagation of a planar reaction-diffusion front, with the products invading the reactants at a constant speed. As the reaction is exothermic, the surface tension γ along the free upper surface varies both with the surface temperature T and with the autocatalytic

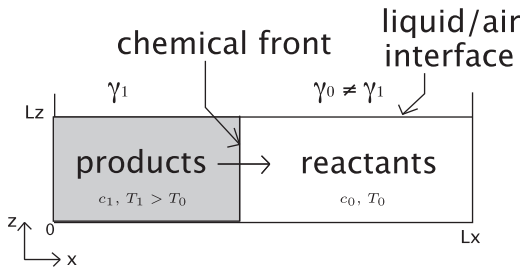

FIG. 1. Schematic of the system.

product concentration c, which can lead to Marangoni-driven convection. We assume that the free surface remains undeformed by the flow since the surface tension is sufficiently strong to keep the liquid surface flat (see Ref. 55 for further comments on this assumption in such systems). We assume that the gas in contact with the free surface has no influence on the dynamics in the liquid layer. Moreover, we neglect possible density variations across the front and focus on Marangoni effects only.

The governing equations are obtained by coupling the incompressible Navier-Stokes equations for the fluid velocity field $\underline{v} = (u, w)$ to reaction-diffusion-convection equations for the evolution of the concentration and temperature fields. We consider a third order reaction kinetics to describe the autocatalytic system, $f(c) = kc^2(a_0 - c)$, with k the rate constant, and a_0 the initial concentration of reactant A. This kinetics is a good description of the IAA reaction known to exhibit front propagation when coupled to diffusion.[3,52,53] The model reads

$$\frac{\partial \underline{v}}{\partial t} + \underline{v}.\nabla\,\underline{v} = \nu\nabla^2\underline{v} - \frac{1}{\rho_0}\underline{\nabla} p + \underline{g}\,, \tag{1}$$

$$\underline{\nabla}\cdot\underline{v} = 0\,, \tag{2}$$

$$\frac{\partial c}{\partial t} + \underline{v}.\underline{\nabla} c = D\nabla^2 c + f(c)\,, \tag{3}$$

$$\rho_0 c_p\left(\frac{\partial T}{\partial t} + \underline{v}.\underline{\nabla} T\right) = \kappa_T\nabla^2 T - \Delta H f(c)\,, \tag{4}$$

where p denotes the pressure, $\underline{g} = (0, -g)$ is the gravity acceleration acting along z. The solution density ρ_0, its kinematic viscosity $\nu = \mu/\rho_0$, where μ is the dynamic viscosity, the molecular diffusion coefficient D, the specific heat capacity of the solution c_p, its thermal conductivity κ_T, the reaction enthalpy ΔH (negative here because the reaction is exothermic), and the kinetic constant k are assumed to be constant.

The velocity vanishes along the bottom wall, assumed to be no-slip. At the free surface, we require $w = 0$ and we use a Marangoni boundary condition for the horizontal fluid velocity u to include the changes in surface tension induced by the gradients of temperature and concentration of the autocatalytic product across the front

$$\mu\frac{\partial u}{\partial z} = \frac{\partial \gamma}{\partial x} = \frac{\partial \gamma}{\partial c}\frac{\partial c}{\partial x} + \frac{\partial \gamma}{\partial T}\frac{\partial T}{\partial x} \quad \text{at} \quad z = L_z\,. \tag{5}$$

We suppose a linear dependence of the surface tension on c and T, $\gamma = \gamma_0 + \partial_c\gamma\, c + \partial_T\gamma\,(T - T_0)$, with γ_0 the surface tension of the initial reactant solution ($c = 0$) at the initial ambient temperature T_0, so that the solutal and thermal coefficients $\partial\gamma/\partial c$ and $\partial\gamma/\partial T$ are assumed constant.

Dimensionless equations are obtained by using the characteristic scales of the reaction-diffusion system: for time, $\tau_c = 1/ka_0^2$, for length, $L_c = \sqrt{D\tau_c}$, for velocity, $U_c = L_c/\tau_c = \sqrt{D/\tau_c}$, and for concentration, a_0. The exothermicity of the reaction leads to an adiabatic temperature rise ΔT in the reaction zone from the ambient temperature T_0 before reaction to $T_0 + \Delta T$, where $\Delta T = -\Delta H a_0/(\rho_0 c_p)$ is positive since the considered autocatalytic reaction is exothermic. Hence, we define a dimensionless temperature as $T' = (T - T_0)/\Delta T$. The pressure is scaled by $p_c = \mu/\tau_c$, so that the dimensionless pressure $p' = p/p_c$. In addition, we define a new pressure gradient incorporating the hydrostatic pressure gradient term as $\underline{\nabla}'p'' = \underline{\nabla}'p' - \rho_0 L_c\underline{g}/p_c$. The dimensionless surface tension is defined as $\gamma' = (\gamma - \gamma_0)/\gamma_c$, with $\gamma_c = \mu\sqrt{D/\tau_c}$. Dropping all the primes, we obtain the following dimensionless governing equations

$$\frac{\partial \underline{v}}{\partial t} + \underline{v}.\nabla\underline{v} = S_c\cdot(-\nabla p + \nabla^2\underline{v})\,, \tag{6}$$

$$\underline{\nabla}\cdot\underline{v} = 0\,, \tag{7}$$

$$\frac{\partial c}{\partial t} + \underline{v}.\underline{\nabla} c = \nabla^2 c + c^2(1 - c)\,, \tag{8}$$

$$\frac{\partial T}{\partial t} + \underline{v}.\underline{\nabla} T = Le\nabla^2 T + c^2(1 - c)\,, \tag{9}$$

where $S_c = \nu/D$ is the Schmidt number and $Le = D_T/D$, the Lewis number, is the ratio between the thermal diffusivity $D_T = \kappa_T/(\rho_0 c_p)$ and the molecular diffusivity D.

The Marangoni boundary condition along the free surface ($z = L_z$) becomes

$$\partial_z u = -Ma_c\partial_x c - Ma_T\partial_x T\,, \tag{10}$$

with the solutal Ma_c and thermal Ma_T Marangoni numbers, defined, respectively, as

$$Ma_c = \frac{-1}{\mu\sqrt{Dk}}\frac{\partial\gamma}{\partial c}\,, \tag{11}$$

$$Ma_T = \frac{-\Delta T}{\mu a_0\sqrt{Dk}}\frac{\partial\gamma}{\partial T}\,, \tag{12}$$

along with no-slip for the vertical component of the velocity and no-flux for the concentration and the temperature:

$$w = \partial_z c = \partial_z T = 0. \tag{13}$$

Indeed, we assume that the system is thermally insulated and the reactor operates adiabatically, therefore neglecting effects of possible heat losses through the system boundaries[57] as well as possible evaporation at the surface. The boundary conditions along the solid bottom boundary ($z = 0$) are no-slip for both velocity components and also no-flux for the concentration and the temperature:

$$u = w = \partial_z c = \partial_z T = 0. \tag{14}$$

We note that the solutal Marangoni number Ma_c is positive if the product decreases the surface tension in the course of reaction and negative otherwise while the thermal Marangoni number Ma_T is always positive since the reaction is exothermic ($\Delta T > 0$) and we work at room temperature where $\partial\gamma/\partial T$ is negative for water. The dimensionless surface tension can therefore be written as

$$\gamma = -Ma_c c - Ma_T T\,. \tag{15}$$

When $T = 1 = c$, the solution corresponds to the hot products of the reaction with a surface tension $\gamma = -Ma_c - Ma_T$, whereas the reactants ($c = 0$) at room temperature ($T = 0$) are characterized by $\gamma = 0$ due to our choice of non-dimensionalization.

Concerning the boundary conditions in the x direction, both periodic boundary conditions (2 fronts) and homogeneous Neumann conditions have been tested. Provided that the front is located far from $x = 0$ and $x = L_x/2$ in the first case and $x = 0$ and $x = L_x$ in the second, the results have been found identical modulo the scheme precision used in each case. Periodic boundary conditions have therefore been used for all the results presented here.

The conservation equations are discretized spatially using spectral elements methods. The domain $[0, L_z] \times [0, L_x]$ is decomposed into N_e macro-elements of size $[0, L_z] \times [iL_x/N_e, (i+1)L_x/N_e]$, where $i \in \{0, ..., N_e - 1\}$. The velocity, pressure, concentration, and temperature fields are approximated by high order interpolant through the Gauss-Lobatto-Legendre points. The time scheme is a time stepping method proposed by Karniadakis *et al.*[58] The results have been validated through comparison with a finite difference method code and with known results of thermal Marangoni convection in non-reactive systems[59] and solutal Marangoni convection around autocatalytic fronts.[1]

B. Reaction-diffusion fronts

In the absence of flow, i.e., for $Ma_c = 0 = Ma_T$, the system of equations (6)–(9) reduces to reaction-diffusion equations for the concentration and the temperature, Eqs. (8) and (9) with $\underline{v} = 0$, respectively. These equations admit as a solution traveling chemical and thermal fronts characterized by a constant propagation speed and a constant width. The concentration follows the analytical profile:[3,52,53]

$$c(x,t) = \frac{1}{1 + e^{(x-vt)/\sqrt{2}}} = \frac{1}{2}\left[1 + \tanh\left(-\frac{\sqrt{2}}{4}(x - vt)\right)\right] \tag{16}$$

where $v = \sqrt{2}/2$ is the constant RD speed of the front. This profile connects the kinetically stable product $c = 1$ to the invaded $c = 0$ solution corresponding to the reactants. The width w_{RD} of this front, defined as the distance between $c = 0.99$ and $c = 0.01$, equals $w_{RD} = 2\sqrt{2}\ln 99 \sim 13$.

As the reaction is exothermic, the traveling concentration front is accompanied by a heat front traveling at the same RD speed v independent of the Lewis number. If $Le = 1$, the solution for the temperature equation (9) is the same as for the concentration equation. However, for aqueous solutions, the Lewis number is larger than one since, in water, heat diffuses faster than mass. For such $Le > 1$, an explicit analytical front solution cannot be found and a numerical integration of Eqs. (8) and (9) with $\underline{v} = 0$ is required to obtain the RD temperature profile. Heat diffusing faster than mass, the width of the temperature front is much larger than the one of the concentration front (see Ref. 56 for further details).

III. MARANGONI CONVECTION AROUND EXOTHERMIC FRONTS

To study the influence of Marangoni effects on the propagation of an exothermic autocatalytic front, we integrate the above equations numerically with step-like initial conditions for the concentration of the autocatalytic product c and the temperature T. The Schmidt number $S_c = \mu/\rho_0 D \sim 10^3$ is computed from the viscosity and the density of water. For D, we use realistic values of the diffusion coefficient of species involved in autocatalytic systems[4,53] ($D \sim 2 \times 10^{-5}\,\mathrm{cm}^2/\mathrm{s}$). In our previous study of solutal Marangoni effects on the propagation of a chemical front,[1] we showed that a change in the value of S_c, if taken in the experimental range, does not affect the obtained results, meaning that inertial effects are negligible in these slow flow regimes compared to the viscous effects. The length of the solution layer is taken long enough for the lateral boundaries not to affect the numerical results, typically $L_x = 300$.

In the remainder of the paper, we will study the influence of the four remaining dimensionless parameters. The solutal Ma_c and thermal Ma_T Marangoni numbers quantify the effect of the chemical reaction and of the exothermicity on the surface tension of the solution. We will vary them in a range similar to our previous study[1] and in particular we will study the effect of the sign of the solutal Marangoni number on the system dynamics. The Lewis number Le, measuring the ratio of thermal and molecular diffusivities, will be varied between 1 and 120 to cover the experimental values in solutions of the IAA reaction[9] ($Le = 70$) and the CT reaction[25] ($Le = 10$), both exothermic reactions leading to the propagation of autocatalytic fronts in spatially extended systems. The effect of the liquid layer thickness on the system dynamics is considered by varying L_z between 2 and 20 while the effect of the other parameters is studied for $L_z = 10$, which corresponds to a one-cm thick solution layer. The dynamics of the system is represented by two-dimensional density plots of the product concentration ranging from $c = 0$ (grey) to $c = 1$ (black). The white color indicates the reaction zone.

A. Spatio-temporal dynamics of the front propagation

If the system is isothermal, the surface tension is a function of the composition only and the Marangoni convection arises from the concentration gradient across the front. We have shown in a previous study that the system evolves towards an asymptotic dynamic regime characterized by a

steady fluid vortex traveling at a constant speed with the front.[1,55] The propagation speed of this front is increased by the presence of natural convection and we observe a pronounced deformation of the front across the layer thickness. There is an asymmetry between the results for positive and negative Marangoni numbers M (same definition as our solutal Marangoni number here, Ma_c, Eq. (11)), which is due to the fact that, for positive M, the flow is initiated at the surface in the same direction as the front propagation whereas the surface flow opposes the front motion for negative M. In both cases, however, the deformation of the front increases with the absolute value of M.

When $Le = 1$, the evolution of the chemical and thermal fronts is described by the same equation (Eq. (8)) and the solutal and thermal effects are therefore additive. The dynamics of an exothermic front characterized by a solutal Marangoni number Ma_c and a thermal Marangoni number Ma_T is identical to the dynamics of an isothermal front[1] characterized by a unique solutal Marangoni number $M = Ma_c + Ma_T$, both for cooperative and antagonistic effects.

However, when $Le > 1$, which is the case in aqueous solutions of the considered autocatalytic reactions, solutal and thermal effects act on different length scales and we need to consider two distinct situations according to the sign of the solutal Marangoni number. We recall that the thermal contribution to the surface tension changes is typically negative ($\Delta T \partial_T \gamma < 0$ and hence $Ma_T > 0$) since propagating autocatalytic fronts are typically exothermic.

1. Cooperative effects: $Ma_c, Ma_T > 0$

When the solutal and thermal Marangoni numbers are both positive, both effects act cooperatively as to decrease the surface tension behind the front, which results in a surface Marangoni flow entraining the hot products towards the zone with the largest surface tension, here the cold reactants. This flow is composed of a positive horizontal flow at the surface and a return flow across the layer, deforming the initially plane chemical front (see Figure 2 for $Ma_c = 20$, $Ma_T = 100$ and $Le = 10$). As in the isothermal case, the system reaches an asymptotic state characterized by a deformed front propagating at a constant speed larger than the RD speed for all Ma_c, Ma_T scanned. Since heat diffuses faster than mass ($Le > 1$), the thermal front is more extended than the solutal front, which leads to temperature gradients smaller than concentration gradients. Consequently, for a same value of the Marangoni number, the thermal effects have a smaller contribution to the decrease of surface tension than the solutal effects and the deformation of an exothermic front characterized by a couple of Marangoni numbers (Ma_c, Ma_T) is weaker than the one of an isothermal front corresponding to a unique Marangoni number $M = Ma_c + Ma_T$.

FIG. 2. Time evolution of the concentration field in the presence of cooperative solutal and thermal Marangoni effects: $Ma_c = 20$ and $Ma_T = 100$. The other parameters are $Le = 10$ and $L_z = 10$.

2. Antagonistic effects: $Ma_c < 0, Ma_T > 0$

The antagonistic situation corresponds to the case when the solutal contribution acts as to increase the surface tension during the reaction whereas the thermal contribution acts as to decrease it since the products are hotter than the reactants. Thermal effects therefore produce a surface flow directed from the products towards the reactants whereas solutal effects act in the reverse direction. Different types of spatio-temporal dynamics can be observed depending on the relative values of Ma_c and Ma_T. Figure 3 illustrates a chemical front when antagonistic Marangoni effects $(Ma_c = -180, Ma_T = 100, Le = 10)$ eventually reach an asymptotic regime, similarly to the cooperative situation. In that case, the products are not hot enough to balance the solutal increase of surface tension during the reaction so that the global surface tension of the products is larger than the one of the reactants. This leads to a surface flow in opposite direction of the front propagation and a counterclockwise recirculating vortex across the layer. The deformed front propagates at a constant speed and with an asymptotic shape that have both been analyzed in detail along with the flow field in the case of isothermal fronts.[1,55]

When the products are hot enough to compensate for the solutal increase of the surface tension, the time evolution of the front can feature periodic succession of non trivial dynamics in a reference frame moving with the front as shown in Figure 4 for $Ma_c = -80, Ma_T = 100$, and $Le = 10$. Starting from a planar front separating the reactants and the products ($t = 0$), the dynamics evolves to a deformed front ($t = 20$). Some of the autocatalytic product is transported by the Marangoni flow along the surface towards the reactant region ($t = 30$–40) where it rapidly invades the layer depth converting the reactants to products ($t = 45$), thereby restoring an almost flat front ($t = 50$), that undergoes the same deformation ($t = 55$) as previously described. This dynamics repeats itself periodically. To shed some light on this "oscillatory dynamics," we remind that, if the Lewis number was equal to one, the surface tension of the products would be smaller than that of the reactants leading to a clockwise

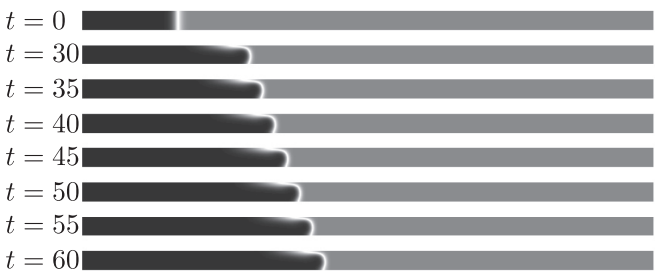

FIG. 3. Time evolution of the concentration field in the presence of antagonistic solutal and thermal Marangoni effects when the system reaches a steady regime propagating at a constant speed: $Ma_c = -180$ and $Ma_T = 100$. The other parameters are $Le = 10$ and $L_z = 10$.

FIG. 4. Periodic time evolution of the concentration field in the presence of antagonistic solutal and thermal Marangoni effects when the front remains unsteady in the co-moving frame: $Ma_c = -80$ and $Ma_T = 100$. The other parameters are $Le = 10$ and $L_z = 10$.

Marangoni vortex deforming the front like in Fig. 2. However, since heat diffuses faster than mass, the products rapidly lose their heat in the reaction zone and we end up with a succession from left to right of hot products, cooled products, heated reactants, and cold reactants. This induces the formation of several vortices across the layer as can be seen in Figure 5(b) showing the streamlines around the deformed front for an unsteady antagonistic situation. Such double diffusive Marangoni effects[61] are thus a key ingredient to understand the periodic unsteady dynamics obtained.

To help understand this, we reconstruct the surface tension along the surface in Figure 6 and compare both the steady and the unsteady situations for $Le = 10$. Figure 6(a) shows that, when $Ma_c = -180$ and $Ma_T = 100$, the surface tension (see Eq. (15)) goes between $-Ma_c - Ma_T = 80$ behind the front (hot products, $c = 1 = T$) and 0 ahead of the front (fresh cold reactants, $c = 0 = T$). The profile of γ is, however, non-monotonic along the surface because in the reaction zone, the reactants on top of the products are heated by the reaction exothermicity and therefore see their surface tension decrease even further. Since a gradient of surface tension along x leads to the formation of a Marangoni vortex, we observe two counter-rotating vortices in the reaction zone for $Ma_c = -180$ and $Ma_T = 100$ (see Fig. 5(a)) related to the two gradients of surface tension with opposite sign shown in Fig. 6(a). The right vortex is weaker since the jump of surface tension between the heated reactants and the cold reactants is smaller than the one between the hot products and the heated reactants. We note that the cooled products region is located in the bulk at the bottom of the deformation zone where they do not contribute to the surface tension changes.

The case of the unsteady dynamics is more complex but can also find an explanation in the surface tension profile along the direction of the front propagation. Figure 6(b)

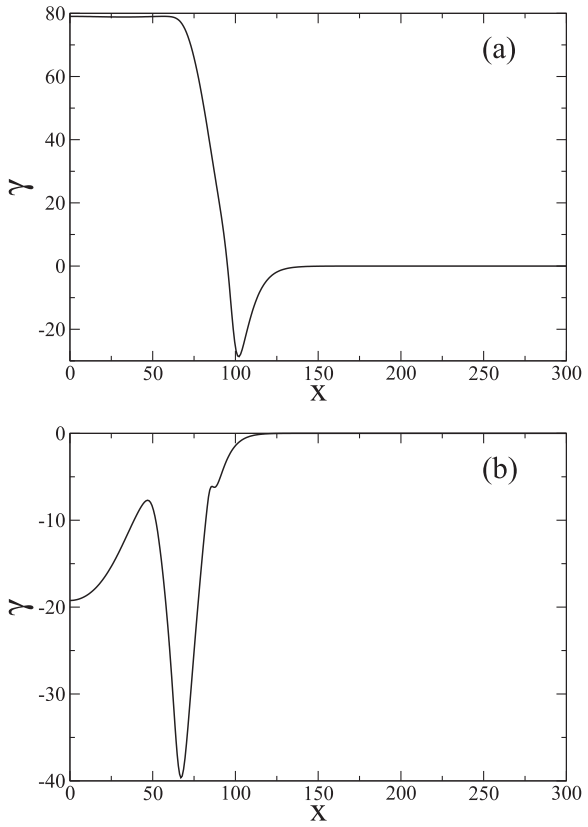

FIG. 6. Surface tension along the surface for $Ma_T = 100$, $Le = 10$, $L_z = 10$, $t = 40$ in (a) a steady antagonistic case, $Ma_c = -180$, and (b) an unsteady antagonistic case, $Ma_c = -80$.

illustrates the spatial dependence of γ for $Ma_c = -80$ and $Ma_T = 100$, going between $-Ma_c - Ma_T = -20$ behind the front to 0 ahead of it. The hot products have a smaller surface tension than the cold reactants thanks to the thermal contribution. In the reaction zone, however, this trend is inverted because heat diffuses faster than mass, leading to a local maximum in γ corresponding to the cooled products and a local (and global) minimum corresponding to the heated reactants. These surface tension gradients can be correlated to the different vortices seen in Fig. 5(b). Oppositely to the previous case discussed in Fig. 6(a), the jump in surface tension between the cold and the heated reactants is the largest, resulting in a strong vortex to the right of the reaction zone. This important flow brings some of the autocatalytic product along, thereby initiating the reaction further ahead (see 3rd, 4th, and 5th panels of Figure 4). Next, the autocatalytic clock reaction rapidly converts the reactants in the nearby zone into products (6th panel), restoring

FIG. 5. Streamlines superimposed on the concentration field in the presence of antagonistic solutal and thermal Marangoni effects for $Ma_T = 100$, $Le = 10$, $L_z = 10$, $t = 40$ for (a) a steady case, $Ma_c = -180$, and (b) an unsteady case, $Ma_c = -80$. The concentration ranges here from $c = 1$ (products to the left) shown in red to $c = 0$ (reactants to the right) shown in blue. The streamlines correspond to iso-contours of the streamfunction, ψ, equally spaced between the maximum value of ψ and 0.

an almost planar front (7th panel) that will undergo the same deformation according to the mechanisms described above (compare 2nd and 8th panels), inducing an oscillatory dynamics. This periodic switch between a deformed front, entrainment of autocatalytic product at the surface, rapid conversion from reactants to products, and return to the initial front results from differential diffusion effects between heat and mass that have antagonistic contributions to the surface tension.

Figure 7 shows another type of unsteady dynamics for $Ma_c = -70, Ma_T = 200$, and $Le = 10$. In this case, the solutal effects tending to increase the surface tension during the reaction are overcome by the thermal effects so that the surface tension of the product is much smaller than the one of the reactants. Even in the reaction zone, the exchange of heat between the products and the reactants is not large enough to invert the surface tension ratio between them and the front is therefore deformed in a similar way as in Figure 2. The fast diffusion of heat, however, leads to a more extended Marangoni vortex around the front and the surface flow entrains some of the autocatalytic product along the surface. As previously described, this initiates the clock reaction ahead of the front, which swiftly converts the fresh reactants into products. In the present case, this does not bring back a planar front because the primary deformation is too extended but the system oscillates between a simple deformation (cf: 2nd panel) and a double deformation of the front (cf: 4th panel).

To summarize the observations, an autocatalytic front propagating in the presence of thermal and solutal Marangoni convection reaches an asymptotic dynamics which is steady in the co-moving frame when both effects are cooperative or in the antagonistic case when the total Marangoni number $Ma_c + Ma_T < M_1$ where M_1 is a threshold value depending on the Lewis number. In the other antagonistic situations, the front oscillates between two states, one with weaker deformation, sometimes almost planar, and the second one with a stronger deformation. We will see further below that steady dynamics can also be observed in the antagonistic case when $Ma_c + Ma_T > M_2$, where M_2 is a second threshold value also function of the Lewis number. In the next section, we characterize the deformation of the front as a function of the Marangoni numbers, the Lewis number, and the layer thickness. We also discuss the domains of existence of the different types of asymptotic dynamics.

FIG. 7. Periodic time evolution of the concentration field in the presence of antagonistic solutal and thermal Marangoni effects when the front remains unsteady in the co-moving frame: $Ma_c = -70$ and $Ma_T = 200$. The other parameters are $Le = 10$ and $L_z = 10$.

B. Characterization of the front deformation

To quantify the deformation of the front across the layer, we define the mixing length W as the distance between $\langle c(x,t)\rangle = 0.01$ and $\langle c(x,t)\rangle = 0.99$, i.e., between the tip and the rear of the transversely averaged concentration profile

$$\langle c(x,t)\rangle = \frac{1}{L_z}\int_0^{L_z} c(x,z,t)dz\,. \tag{17}$$

Figure 8 shows the temporal evolution of the mixing length for $Ma_T = 100, Le = 10, L_z = 10$, and various solutal Marangoni numbers ranging from $Ma_c = -180$ (steady antagonistic case with $Ma_c + Ma_T < M_1$) to $Ma_c = 20$ (steady cooperative case). In all the cases presented, the mixing length either converges to a constant value function of the parameters of the system in the case of steady regimes or oscillates with a constant amplitude between a minimum and a maximum deformation, also depending on the parameter values. In the remainder of the paper, we refer to the mixing length as either the asymptotic value of W reached when the asymptotic dynamics is steady or as the two values characterizing the minimum and maximum mixing lengths, respectively, when the asymptotic dynamics is oscillatory.

1. Influence of the Marangoni numbers

At fixed $Le = 10$, the domains of existence of the different types of asymptotic dynamics depend on the relative strength of the solutal and thermal effects and therefore on the values of the couple (Ma_c, Ma_T). Figure 9 illustrates the variation of the mixing length with Ma_c for various Ma_T. First, we note that if $Ma_T = 0$, the exothermicity of the reaction does not contribute to the changes in surface tension and the induced Marangoni flow field is therefore identical to the one driven by solutal effects in the isothermal case. The curve for $Ma_T = 0$ is hence the same as in Figure 17(a) of our previous study,[1] showing that the deformation of the front increases with the absolute value of the solutal Marangoni number, which quantifies the effect of a concentration gradient on the surface tension, and that the results are asymmetric between positive and negative Ma_c.

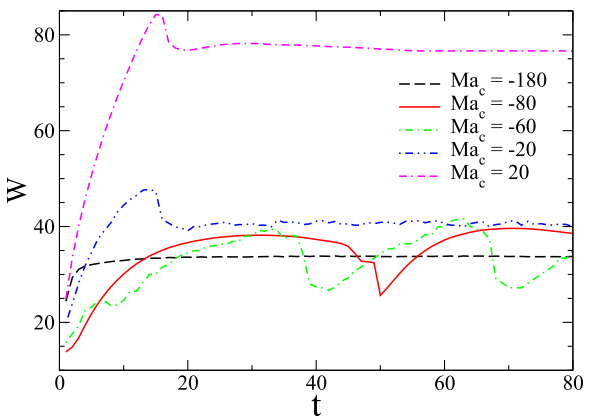

FIG. 8. Mixing length as a function of time for $Ma_T = 100$, $Le = 10$, $L_z = 10$, and various $Ma_c = -180, -80, -60, -20, 20$.

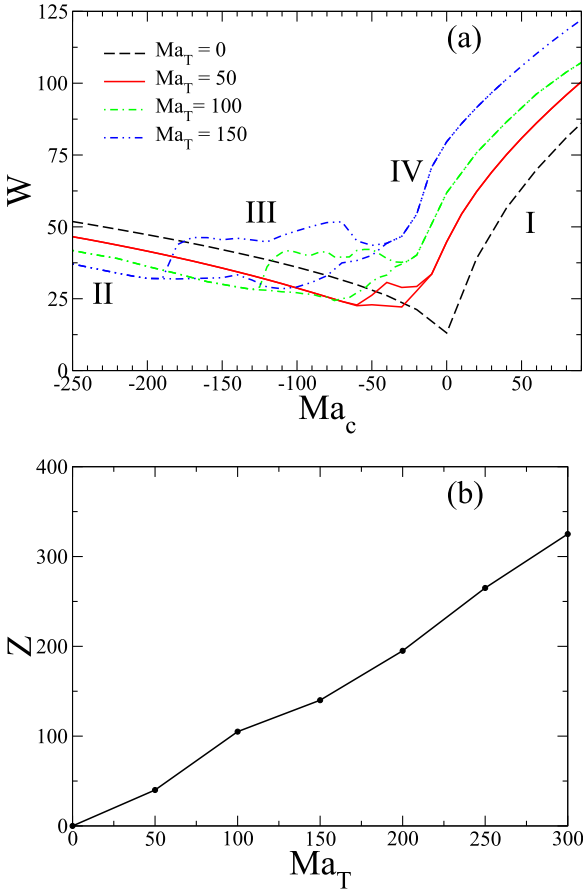

FIG. 9. (a) Mixing length as a function of Ma_c for $Le = 10$ and various $Ma_T = 0, 50, 100, 150$. Zones where the curve is splitted correspond to situations where the front is unsteady in the co-moving frame. (b) Solutal Marangoni range, Z, for which the front is unsteady as a function of Ma_T. In both figures, the thickness of the layer is $L_z = 10$.

When $Ma_T \neq 0$, we need to distinguish between the four different situations illustrated in Figure 9. (1) If $Ma_c > 0$, the solutal and thermal effects are cooperative (zone I, cf: Fig. 2). The system attains a steady dynamics, and the constant mixing length increases with both Ma_c and Ma_T. (2) If $Ma_c < 0$, with $Ma_c + Ma_T$ sufficiently small, $(Ma_c + Ma_T < M_1)$, i.e., $|Ma_c + Ma_T|$ large solutal and thermal effects are antagonistic and the asymptotic dynamics is steady (zone II). Solutal effects are dominating and the front is deformed by a counter-clockwise Marangoni vortex (cf: Fig. 3). Inside this zone, the mixing length increases with the absolute value of Ma_c, which increases the surface tension difference between the products and the reactants. On the other hand, W decreases with Ma_T because the thermal effects contribute to reduce this surface tension gradient. The size of this region decreases with Ma_T since the larger Ma_T, the smaller Ma_c has to be to dominate the thermal effects. (3) If $Ma_c < 0$, with intermediate $Ma_c + Ma_T$ $(M_1 < Ma_c + Ma_T < M_2)$, the dynamics is oscillatory (zone III, cf: Figs. 4 and 7). The amplitude of the oscillations increases with Ma_T as well as the solutal Marangoni range, $Z = M_2 - M_1$, for which these oscillations are observed (see Fig. 9(b)). (4) If $Ma_c < 0$, with $Ma_c + Ma_T$ large enough $(Ma_c + Ma_T > M_2)$, the asymptotic dynamics is steady again (zone IV). In this case, thermal effects are dominating and the front is deformed by a clockwise vortex similarly to the cooperative situation. The deformation of the front increases with both Marangoni numbers (meaning a smaller solutal effect since $Ma_c < 0$), which corresponds to an increase of the surface tension difference across the front. The size of this region where thermal effects dominate accordingly increases with Ma_T.

2. Influence of the Lewis number

The Lewis number measures the ratio between thermal and molecular diffusivities. Figure 10 depicts the influence of Le on the front deformation characterized by W. When $Le = 1$, the solutal and thermal effects are simply additive and W behaves like in the isothermal case with $M = Ma_c + Ma_T$. The curve is therefore here shifted by $-Ma_T$ with respect to the isothermal curve.[1] When $Le \to \infty$, the isothermal case is recovered because heat diffusion is so large that the thermal effects are negligible and the description of the system tends to the unshifted isothermal curve (see $W(Ma_c)$ for $Le = 120$). For intermediate Le, the four asymptotic regimes described in Fig. 9 are observed. The amplitude of the oscillations as well as the Ma_c range delimiting the oscillatory region, Z, are non-monotonous functions of Le (see Fig. 10(b)). The existence of a maximum arises from the fact that Le needs to be large enough to

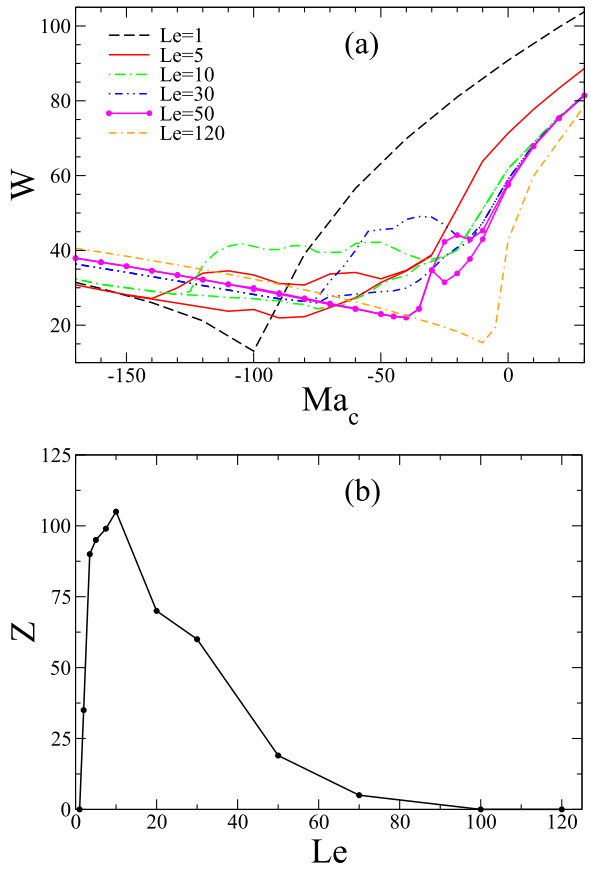

FIG. 10. (a) Mixing length as a function of Ma_c for $Ma_T = 100$ and various $Le = 1, 5, 10, 30, 50, 120$. Zones where the curve is splitted correspond to situations where the front is unsteady in the co-moving frame. (b) Solutal Marangoni range, Z, for which the front is unsteady as a function of Le when $Ma_T = 100$. In both figures, the thickness of the layer is $L_z = 10$.

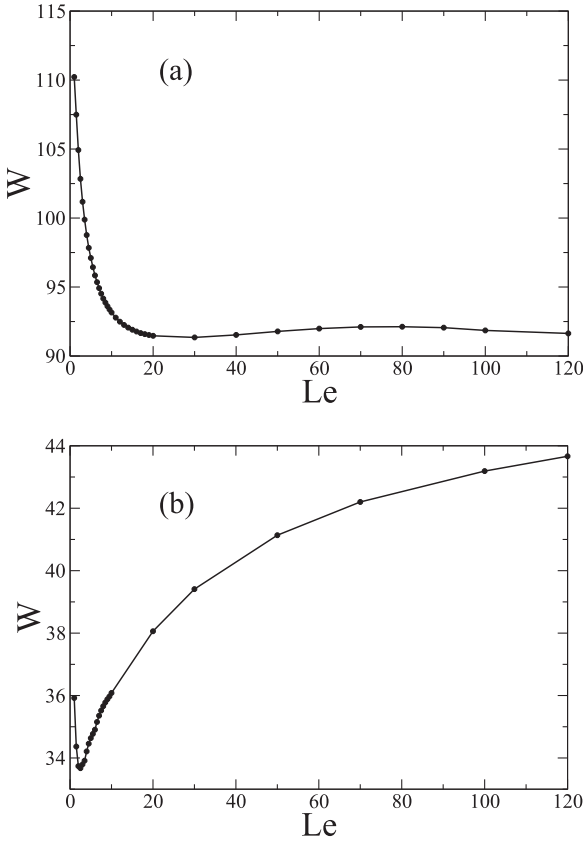

FIG. 11. Mixing length as a function of Le for $Ma_T = 100$ and $L_z = 10$, in (a) the cooperative case, $Ma_c = 50$, and (b) the antagonistic case, $Ma_c = -200$.

induce a significant oscillatory mechanism but not too large to prevent heat from diffusing too far ahead thereby suppressing this mechanism. There is therefore an optimal Le ($Le_{\text{opt}} \sim 10$ for $Ma_T = 100$) for which oscillations are observed for the largest range of Ma_c.

Figure 11 shows the influence of Le on the mixing length in both cooperative and antagonistic steady regimes. When Le increases at fixed positive Ma_c and Ma_T, the same surface tension jump between the products and the reactants is stretched out on a wider region since heat diffuses faster. This results in a weaker Marangoni flow and therefore a smaller deformation of the front. At large $Le \sim 80$, the presence of a local maximum might be explained by the fact that when Le increases, the region where flow is present is larger, which is negligible at small Le but might contribute to the front spreading at large Le. In the antagonistic case, W goes non-monotonically from 36 at $Le = 1$ (cf: isothermal value for $M = Ma_c + Ma_T = -100$) to 43.5 at $Le = 120$ (tending to the isothermal value $W = 50$ for $M = Ma_c = -200$). Since thermal effects reduce the surface tension jump across the front and larger Le smear out this effect, W increases with $Le > 2.5$. The presence of a minimum at $Le = 2.5$ remains, however, unclear.

3. Influence of the layer thickness

Figure 12 shows the mixing length increasing with the layer thickness for both cooperative and antagonistic steady cases. As in the isothermal case,[60] this can be explained by the presence of the bottom no-slip boundary. For a same surface tension gradient, the maximum flow velocity will

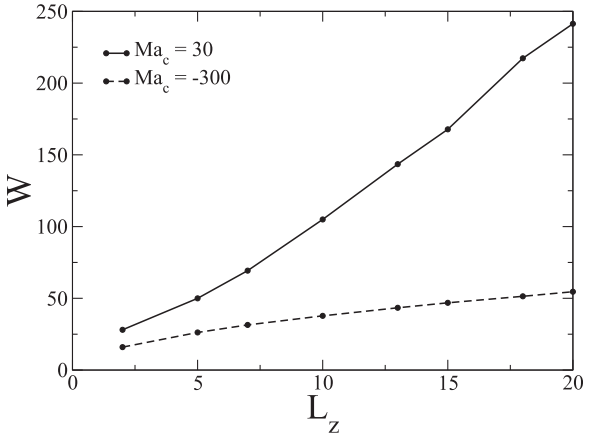

FIG. 12. Mixing length as a function of the layer thickness for $Ma_T = 200$ and $Le = 10$ in both a cooperative ($Ma_c = 30$) and a steady antagonistic ($Ma_c = -300$) case.

increase with L_z because the system is less influenced by the zero velocity condition at the bottom.

IV. CONCLUSION

We have numerically studied the dynamics of an exothermic autocatalytic front propagating horizontally in the presence of Marangoni-driven convection. The surface tension gradient across the front can have a solutal origin linked to the changes in concentration and a thermal source arising from the reaction exothermicity. In isothermal conditions, the system has been shown to exhibit asymptotic dynamics featuring a steady fluid vortex propagating at a constant speed with the deformed front.[1,55] We have here quantified the additional influence of thermal effects on such frontal dynamics. In that case, the surface tension jump across the front has both a solutal and a thermal contribution. In the case of the exothermic autocatalytic reactions studied, the thermal contribution to the surface tension difference is always negative since the heat produced by the reaction acts as to decrease the surface tension. The solutal contribution, however, can have both signs depending if the compositional changes increase or decrease the surface tension in the course of the reaction.

When both effects act as to decrease the surface tension during the reaction, the dynamics is referred to as cooperative and the system attains an asymptotic regime similar to the isothermal situation. In the case of antagonistic effects, new dynamics can be observed if both effects act on different length scales. The difference in diffusivities of heat and mass triggers indeed new phenomena such as an oscillatory dynamics characterized by the periodic alternation between a deformed front, the spreading of autocatalytic product entrained by the thermal Marangoni flow at the surface, and the rapid transformation of reactants into products restoring the weakly deformed front. We note that oscillations of the concentration field have also been observed in the case of antagonistic solutal and thermal effects in the case of pure buoyancy-driven flows.[44,56] The explanation involves, however, different mechanisms since only surface forces are present here.

We have characterized the system dynamics as a function of the Marangoni numbers, quantifying the effect of concentration and temperature gradients on the surface tension, of the Lewis number, measuring the ratio between thermal and molecular diffusivities, and of the layer thickness. We have shown that the deformation of the front by the Marangoni-driven flow increases with the absolute value of the total Marangoni number, $|Ma_c + Ma_T|$, and with the layer thickness. When both effects act cooperatively, the front deformation decreases with Le which reflects the spreading of the thermal front, and hence of the surface tension gradient. When both effects contribute antagonistically, several regimes (steady counter-clockwise vortex, steady clockwise vortex, and oscillatory dynamics) have been obtained and characterized as a function of Ma_c, Ma_T, and Le.

In conclusion, this work has contributed to a systematic investigation of the various effects involved in the dynamics of chemical fronts propagating in horizontal solution layers with a free surface by considering the influence of pure solutal and thermal Marangoni effects on the frontal dynamics.

ACKNOWLEDGMENTS

Financial support by ESA, FNRS, and Prodex is gratefully acknowledged. L.R. is supported by the F.R.S.-FNRS Belgium.

[1]L. Rongy and A. De Wit, J. Chem. Phys. **124**, 164705 (2006).
[2]G. Nicolis and I. Prigogine, *Self-Organization in Nonequilibrium Systems* (Wiley, New York, 1977).
[3]*Oscillations and Traveling Waves in Chemical Systems*, edited by R. J. Field and M. Burger (Wiley, New York, 1985).
[4]I. R. Epstein and J. A. Pojman, *An Introduction to Nonlinear Chemical Dynamics* (Oxford University Press, Oxford, 1998).
[5]W. van Saarloos, Phys. Rep. **386**, 29 (2003).
[6]G. Bazsa and I. R. Epstein, J. Phys. Chem. **89**, 3050 (1985).
[7]I. Nagypál, G. Bazsa, and I. R. Epstein, J. Am. Chem. Soc. **108**, 3635 (1986).
[8]J. A. Pojman and I. R. Epstein, J. Phys. Chem. **94**, 4966 (1990).
[9]J. A. Pojman, I. R. Epstein, T. J. McManus, and K. Showalter, J. Phys. Chem. **95**, 1299 (1991).
[10]D. A. Vasquez, J. W. Wilder, and B. F. Edwards, J. Chem. Phys. **98**, 2138 (1993).
[11]J. Masere, D. A. Vasquez, B. F. Edwards, J. W. Wilder, and K. Showalter, J. Phys. Chem. **98**, 6505 (1994).
[12]H. Miike and S. C. Müller, Chaos **3**, 21 (1993).
[13]M. J. B. Hauser and R. H. Simoyi, Chem. Phys. Lett. **227**, 593 (1994).
[14]K. Matthiessen and S. C. Müller, Phys. Rev. E **52**, 492 (1995).
[15]S. Kai, T. Ariyoshi, S. Inanaga, and H. Miike, Physica D **84**, 269 (1995).
[16]T. Sakurai, E. Yokoyama, and H. Miike, Phys. Rev. E **56**, 2367 (1997).
[17]O. Inomoto, S. Kai, T. Ariyoshi, and S. Inanaga, Int. J. Bifurcation Chaos Appl. Sci. Eng. **7**, 989 (1997).
[18]B. S. Martincigh and R. H. Simoyi, J. Phys. Chem. A **106**, 482 (2002).
[19]M. Böckmann and S. C. Müller, Phys. Rev. Lett. **85**, 2506 (2000).
[20]A. De Wit, Phys. Rev. Lett. **87**, 054502 (2001).
[21]D. Horváth, T. Bánsági, Jr., and A. Tóth, J. Chem. Phys. **117**, 4399 (2002).
[22]J. Martin, N. Rakotomalala, D. Salin, and M. Böckmann, Phys. Rev. E **65**, 051605 (2002).
[23]R. Demuth and E. Meiburg, Phys. Fluids **15**, 597 (2003).
[24]A. De Wit, Phys. Fluids **16**, 163 (2004).
[25]T. Bánsági, Jr., D. Horváth, Á. Tóth, J. Yang, S. Kalliadasis, and A. De Wit, Phys. Rev. E **68**, 055301(R) (2003).
[26]T. Tóth, D. Horváth, and Á. Tóth, Chem. Phys. Lett. **442**, 289 (2007).
[27]L. Šebestíková, J. D'Hernoncourt, M. J. B. Hauser, S. C. Müller, and A. De Wit, Phys. Rev. E **75**, 026309 (2007).
[28]J. D'Hernoncourt, A. Zebib, and A. De Wit, Chaos **17**, 013109 (2007).
[29]P. Grosfils, F. Dubois, C. Yourassowsky, and A. De Wit, Phys. Rev. E **79**, 017301 (2009).
[30]I. P. Nagy, A. Keresztessy, J. A. Pojman, G. Bazsa, and Z. Noszticzius, J. Phys. Chem. **98**, 6030 (1994).
[31]A. Keresztessy, I. P. Nagy, G. Bazsa, and J. A. Pojman, J. Phys. Chem. **99**, 5379 (1995).
[32]G. Schuszter, T. Tóth, D. Horváth, and Á. Tóth, Phys. Rev. E **79**, 016216 (2009).
[33]N. Jarrige, I. Bou Malham, J. Martin, N. Rakotomalala, D. Salin, and L. Talon, Phys. Rev. E **81**, 066311 (2010).
[34]É. Pópity-Tóth, D. Horváth, and Á. Tóth, J. Chem. Phys. **135**, 074506 (2011).
[35]T. Plesser, H. Wilke, and K. H. Winters, Chem. Phys. Lett. **200**, 158 (1992).
[36]D. A. Vasquez, J. M. Littley, J. W. Wilder, and B. F. Edwards, Phys. Rev. E **50**, 280 (1994).
[37]H. Wilke, Physica D **86**, 508 (1995).
[38]Y. Wu, D. A. Vasquez, B. F. Edwards, and J. W. Wilder, Phys. Rev. E **51**, 1119 (1995).
[39]L. Rongy, N. Goyal, E. Meiburg, and A. De Wit, J. Chem. Phys. **127**, 114710 (2007).
[40]M. A. Budroni, M. Masia, M. Rustici, N. Marchettini, V. Volpert, and P. C. Cresto, J. Chem. Phys. **128**, 111102 (2008).
[41]I. Bou Malham, N. Jarrige, J. Martin, N. Rakotomalala, L. Talon, and D. Salin, J. Chem. Phys. **133**, 244505 (2010).
[42]J. A. Pojman, R. Craven, A. Khan, and W. West, J. Phys. Chem. **96**, 7466 (1992).
[43]M. Belk, K. G. Kostarev, V. Volpert, and T. M. Yudina, J. Phys. Chem B **107**, 10292 (2003).
[44]L. Rongy, G. Schuszter, Z. Sinkó, T. Tóth, D. Horváth, A. Tóth, and A. De Wit, Chaos **19**, 023110 (2009).
[45]T. Rica, É. Pópity-Tóth, D. Horváth, and Á. Tóth, Physica D **239**, 831 (2010).
[46]O. Miholics, T. Rica, D. Horváth, and Á. Tóth, J. Chem. Phys. **135**, 204501 (2011).
[47]L. Sebestíková and M. J. B. Hauser, Phys. Rev. E **85**, 036303 (2012).
[48]Z. Dagan and C. Maldarelli, Chem. Eng. Sci. **42**, 1259 (1987).
[49]L. M. Pismen, Phys. Rev. Lett. **78**, 382 (1997).
[50]K. Matthiessen, H. Wilke, and S. C. Müller, Phys. Rev. E. **53**, 6056 (1996).
[51]M. Diewald, K. Matthiessen, S. C. Müller, and H. R. Brand, Phys. Rev. Lett. **77**, 4466 (1996).
[52]A. Hanna, A. Saul, and K. Showalter, J. Am. Chem. Soc. **104**, 3838 (1982).
[53]K. Showalter, in *Kinetics of Nonhomogenous Processes*, edited by G. R. Freeman (Wiley, New York, 1987), p. 769.
[54]D. Horváth and K. Showalter, J. Chem. Phys. **102**, 2471 (1995).
[55]L. Rongy, A. De Wit, and G. M. Homsy, Phys. Fluids **20**, 072103 (2008).
[56]L. Rongy and A. De Wit, J. Chem. Phys. **131**, 184701 (2009).
[57]J. D'Hernoncourt, S. Kalliadasis, and A. De Wit, J. Chem. Phys. **123**, 234503 (2005).
[58]G. E. Karniadakis, M. Israeli, and S. A. Orszag, J. Comput. Phys. **97**, 414 (1991).
[59]A. A. Nepomnyashchy, M. G. Velarde, and P. Colinet, *Interfacial Phenomena and Convection* (Chapman and Hall/CRC, Boca Raton, 2002).
[60]L. Rongy and A. De Wit, J. Eng. Math. **59**, 221 (2007).
[61]J. Zhan, Z. Chen, Y. Li, and Y. Nie, Phys. Rev. E. **82**, 066305 (2010).